This is a previous version of the article published in Journal of Vibration Engineering & Technologies. 2024. https://doi.org/10.1007/s42417-023-01263-2

Flatness-based control in successive loops of an H-type gantry crane with dual PMLSM

G. Rigatos[a] P. Siano[b] M. AL-Numay[c]

[a]Unit Industrial Autom.
Industrial Systems Inst.
26504, Patras, Greece
grigat@ieee.org

[b]Dept. Innovation Syst.
University of Salerno
Fisciano, 84084, Italy
psiano@unisa.it

[c]Electrical Eng. Dept
King Saud University
Riyadh 11421, Saudi Arabia
alnumay@ksu.edu.sa

M. Abbaszadeh[d] J. Pomares[e] G. Cuccurullo[f]

[d]Dept.ECS Engineering
Rensselaer Polytechnic Inst.
12065, NY, USA
masouda@ualberta.ca

[e]Dept. Systems Eng.
Univ. of Alicante
03690, Alicante, Spain
jpomares@gcloud.ua.es

[f]Dept. Industrial Eng.
Univ. of Salerno
Fisciano, 84084, Italy
gcuccurullo@unisa.it

Abstract: Gantry cranes of the H-type with dual electric-motor actuation are widely used in industry. In this article the control problem of an H-type gantry crane which is driven by a pair of linear permanent magnet synchronous motors is considered. The integrated system that comprises the H-type gantry crane and its two PMLSMs is shown to be differentially flat. The control problem for this robotic system is solved with the use of a flatness-based control approach which is implemented in successive loops. To apply flatness-based control in successive loops, the state-space model of the H-type gantry crane with dual PMLSM is separated into subsystems, which are connected in cascading loops. Each one of these subsystems can be viewed independently as a differentially flat system and control about it can be performed with inversion of its dynamics as in the case of input-output linearized flat systems. The state variables of the preceding (i-th) subsystem become virtual control inputs for the subsequent (i+1-th) subsystem. In turn, exogenous control inputs are applied to the last subsystem. The whole control method is implemented in successive loops and its global stability properties are also proven through Lyapunov stability analysis. The proposed method achieves stabilization of the H-type gantry crane with dual PMLSM without the need of diffeomorphisms and complicated state-space model transformations.

Keywords: H-type gantry cranes, Linear Permanent Magnet Synchronous Motors, differential flatness properties, flatness-based control in successive loops, global stability, Lyapunov analysis.

1 Introduction

In this article, the feedback control and stabilization problem of dual PMLSM-driven H-type gantry cranes is treated with the use of flatness-based control method which is implemented in successive loops. Differential flatness theory and flatness-based control are currently main research directions in the area of nonlinear dynamical systems [1-8]. A system is considered to be differentially flat if (i) all its state variables and its control inputs can be written as differential functions of a subset of its state vector elements which constitute the systems' flat outputs, (ii) the flat outputs of the system are differentially independent which

means that they are not connected through a relation in the form of an homogenous differential equation [9-12]. The differential flatness property is a constrained controllability condition, since it demonstrates that there exist control inputs which enable the state vector elements track precisely the setpoints associated with them . Besides, by proving that a dynamical system is differentially flat it is also confirmed that it can be transformed into the input-output linearized form and subsequently into the canonical Brunovsky from through successive differentiations of its flat outputs [13-17]. By exploiting this latter property, the majority of flatness-based controllers is designed. The controlled system is written into the canonical Brunovsky form through consecutive differentiations of its flat outputs, and this latter state-space form is both controllable and observable [18-21]. Using this new state-space description the feedback control and state estimation problems are treated.

However, flatness-based control through descriptions into the input-output linearized form and the canonical Brunovsky form requires also inverse transformation for finding the control inputs which should be applied to the initial nonlinear state-space model of the system. These inverse transformations may come against non-invertibility (singularity) issues. To overcome the need for state-space model transformations and to exclude the occurrence of singularities in the computation of the control inputs, the present article develops a flatness-based control method in successive loops [22-25]. To this end, the dynamic model of the dual-PMLSM-driven gantry crane is decomposed into a series of subsystems which are connected in chained form. It is proven that, each one of these subsystems, if viewed independently is differentially flat. The state vector of the subsequent $i+1$-th subsystem is considered to be a virtual control input for the preceding i-th subsystem. Equivalently, the virtual control inputs vector of the preceding i-th subsystem is considered to be the setpoints vector of the subsequent $i+1$-th subsystem. From the last N-th subsystem the real control inputs of the gantry crane are computed by tracing backwards all preceding subsystems $N-1, \cdots, 1$. The real control inputs signal contained also recursively the virtual control inputs of all preceding subsystems $1, \cdots, N-1$. Despite its simplicity, the flatness-based control method in successive loops performs remarkably well and achieves also fast and accurate tracking of setpoints by the state variables of the gantry crane. Using the local differential flatness properties of each one of the individual subsystems the design of a local stabilizing feedback controller becomes an easy procedure. It suffices to invert the dynamics of each subsystem, as it is often done for input-output linearizable systems while it also suffices the control input for each subsystem to comprise a diagonal feedback gains matrix with positive diagonal elements. The global stability properties of the new control method are also proven through Lyapunov analysis.

The present article proposes flatness-based control in successive loops for dual-PMLSM-driven gantry cranes. Dual-drive H-type gantry cranes are long-stroke high-speed Cartesian robotic systems which can be used in several industrial applications, such as (i) circuit assembly, printing circuit boards, photolithography, (ii) precision machining, computer numerical control (CNC), arc welding and laser or plasma cutting, (iii) as lifting machines and for the loading, unloading and transfer of cargos, and finally (iv) in biomedical applications such as CT and X-ray scanning [26-28]. The dual-drive H-type gantry crane consists of two linear motors which are arranged in parallel along the vertical axes of an orthogonal board and which are rigidly connected with a cross-beam along the horizontal axis [29- 31] . Dual drive gantry cranes can achieve high torque and high precision in tasks' execution [32-34]. The cross-beam serves also as support to a third linear motor carrying a load [35-38]. There is need for precise synchronization between the two parallel motors and for minimization of internal forces [39- 42]. When the two linear motors are not well synchronized the crossbeam will mis-align from the horizontal axis and will rotate by a small angle around its center of gravity [43-45]. Synchronization error is often caused by unbalanced forces, mechanical assembly variations and various disturbances [46-48]. Permanent Magnet Linear Synchronous Motors (PMLSMs) are a core subsystem in H-type gantry cranes [49-52]. PMLSMs can generate the actuation forces which enable precise positioning along the crane's vertical and the horizontal axes [53-55]. Taking into account the above, the use of flatness-based control in successive loops in the dynamic model of the dual-PMLSM-driven gantry crane is a challenging research topic.

The structure of the article is as follows: In Section 2 the dynamic model of the dual PMLSM-driven gantry crane is analyzed and the associated state-space model is formulated. It is proven that this robotic system is differentially flat. In Section 3 it is demonstrated that the state-space model of the dual-PMLSM-driven gantry crane can be decomposed into a series of chained subsystems. It is also proven that if each one of these subsystems is viewed independently it is also differentially flat. In Section 4 flatness-based control in successive loops is developed for the dynamic model of the dual PMLSM-driven gantry crane. The global stability of the multi-loop flatness-based control method is also proven through Lyapunov analysis. In Section 5 the performance of the flatness-based control method in successive loops for the dynamic model of the dual-PMLSM-driven gantry crane is tested through simulation experiments. Finally, in Section 6 concluding remarks are stated.

2 Dynamic model of the dual PMLSM-driven H-type gantry crane

The diagram of the dual-drive H-type gantry crane with actuation by two Permanent Magnet Linear Synchronous Motors is given in Fig. 2. The model of the gantry crane comprises four masses which are defined as follows: (i) m_b is the mass of the beam, (ii) m_h is the mass of the moving head (load), (iii) m_1 the mass of the first motor, (iv) m_2 the mass of the second motor. The motion of the gantry crane is also defined by four friction coefficients: (i) c_{g_1} is the friction coefficient of the first motor which moves at velocity $\dot{X}_1$, (ii) c_{g_2} is the friction coefficient of the second motor which moves at velocity $\dot{X}_2$, (iii) c_y is the friction coefficient for the actuator that moves the load along the rigid beam, (iv) $c_b = c_{b_1} + c_{b_2}$ is the friction coefficient of the beam, which is connected to the two motors with two flexible joints that exhibit friction coefficients c_{b_1} and c_{b_2} respectively. There is also a stiffness coefficient for the beam which is defined as $k_b = k_{b_1} + k_{b_2}$. The beam has length l_b. The head (load) has length l_h [26], [40].

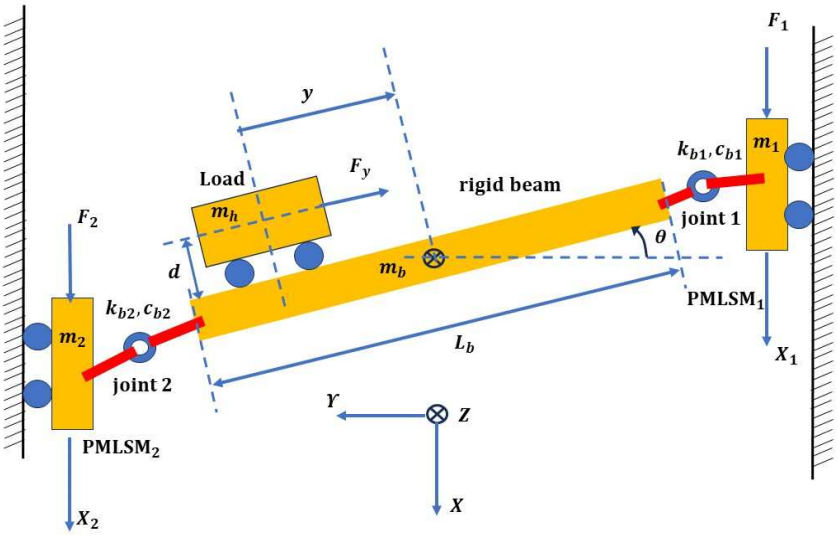

Figure 1: Diagram of the dual-drive H-type gantry crane with actuation by two Permanent Magnet Linear Synchronous Motors

The position of motor 1 is denoted as X_1, while the position of motor 2 is denoted as X_2. The position of

the load with respect to the center of mass of the beam is denoted as Y. Moreover, the following position variables are defined

$$\begin{pmatrix} X \\ \Theta \\ Y \end{pmatrix} = \begin{pmatrix} \frac{1}{2} & \frac{1}{2} & 0 \\ \frac{1}{L_b} & -\frac{1}{L_b} & 0 \\ 0 & 0 & 1 \end{pmatrix} \begin{pmatrix} X_1 \\ X_2 \\ Y \end{pmatrix} \tag{1}$$

Using the Euler-Lagrange approach, the dynamic model of the dual gantry crane is [40], [5]

$$M\ddot{q} + H\dot{q} + C\dot{q} + Kq = F \tag{2}$$

where $q = [X, \Theta, Y]^T$ is the state vector of the crane. The inertia matrix $M(q)$ is [40]

$$M = \begin{pmatrix} M_{11} & M_{12} & -m_b sin(\theta) \\ M_{12} & J_t + m_b Y^2 & -m_h d \\ -m_b sin(\Theta) & -m_b d & m_b \end{pmatrix} \tag{3}$$

where $J_t = J_b + J_h + 0.25(m_1 + m_2)L_b + m_h d^2$ with J_b to be the moment of inertia of the beam and J_h to be the moment of inertia of the load. Moreover, $M_{11} = m_1 + m_2 + m_b + m_h$ and $M_{12} = m_h d \cdot sin(\Theta) - [m_h Y - 0.5(m_1 - m_2)L_b]cos(\Theta)$.

Matrix H is the Coriolis and centrifugal forces matrix: [40]

$$H = \begin{pmatrix} 0 & H_{12}\dot{\Theta} & -2m_b\dot{\Theta}cos(\Theta) \\ 0 & 2m_b Y\dot{Y} & 0 \\ 0 & -m_b Y\Theta & 0 \end{pmatrix} \tag{4}$$

Matrix K is the damping forces matrix which is defined as

$$K = \begin{pmatrix} 0 & 0 & 0 \\ 0 & K_{22} & 0 \\ 0 & 0 & 0 \end{pmatrix} \tag{5}$$

where $K_{22} = K_{b_1} + K_{b_2}$. The generalized forces vector is

$$F = \begin{pmatrix} F_c & M_c & F_y \end{pmatrix}^T \tag{6}$$

where F_c is a force causing translation X of the beam, M_c is a torque causing rotation of the beam by angle Θ and F_y is a force causing translation of the load. The relation connecting the generalized forces vector to the forces generated by the PMLSMs of the gantry crate are [40]

$$\begin{pmatrix} F_c \\ M_c \\ F_y \end{pmatrix} = \begin{pmatrix} 1 & 10 & \\ \frac{L_b}{2} & -\frac{L_b}{2} & 0 \\ 0 & 0 & 1 \end{pmatrix} \begin{pmatrix} F_1 \\ F_2 \\ F_y \end{pmatrix} \tag{7}$$

The above relation about the forces vectors of the gantry crane can be also written as

$$F = A_F F_1 \tag{8}$$

About the moments of inertia of the crane it holds that $J_b = m_b \frac{L_b^2}{12}$ and $J_h = m_h \frac{L_b^2}{12}$.

Using description of the voltage and current variables of the PMLSM in the dq reference frame, the dynamics of each motor is given by [2]

$$\begin{aligned} \dot{i}_q &= -i_q \frac{R_s}{L_q} - \frac{n_p \pi v}{L_q \tau}(L_d i_d + \lambda_{pm}) + \frac{1}{L_q} v_q \\ \dot{i}_d &= -i_d \frac{R_s}{L_d} - \frac{n_p \pi v}{L_d \tau} L_q i_q + \frac{1}{L_d} v_d \end{aligned} \tag{9}$$

The parameters of the electric part of the PMLSM are: R_s is the motor's resistance, λ_{pm} is the magnetic flux due to permanent magnets, n_p is the number of poles of the motor, L_d, L_q are the dq frame inductances. Moreover, i_d, i_q are the dq frame current variables, and v_d, v_q are the dq frame voltage input variables. Additionally v is the linear velocity of the moving part of each PMLSM. For the first motor this velocity variable is $\dot{X}_1$, for the second motor it is $\dot{X}_2$ and for the motor moving the load it is $\dot{Y}$. The electromagnetic force for each motor is

$$F_e = \frac{3\pi n_p}{M+M_L}\frac{\lambda_{pm} i_q - (L_d - L_q) i_d i_q}{2\tau} - Dv \tag{10}$$

and by considering that $L_d = L_q$ and a small friction coefficient $D = 0$ the electromagnetic force of the motor is given by

$$F_e = \frac{3\pi n_p}{M+M_L}\frac{\lambda_{pm}}{2\tau} i_q \tag{11}$$

Next, the dynamic model of the dual-drive H-type gantry crane is written as

$$\begin{gathered} \ddot{q} = -M^{-1}H\dot{q} - M^{-1}C\dot{q} - M^{-1}Kq + M^{-1}A_f F_1 \Rightarrow \\ \ddot{q} = -M^{-1}(H+C)\dot{q} - M^{-1}Kq + M^{-1}A_f F_1 \end{gathered} \tag{12}$$

About the inverse of the inertia matrix M of the dual-drive gantry crane it holds that

$$M^{-1} = \frac{1}{detM}\begin{pmatrix} \bar{M}_{11} & -\bar{M}_{21} & \bar{M}_{31} \\ -\bar{M}_{12} & \bar{M}_{22} & -\bar{M}_{32} \\ \bar{M}_{13} & -\bar{M}_{23} & \bar{M}_{33} \end{pmatrix} \tag{13}$$

where $\bar{M}_{11} = (J_t + m_b Y^2)m_b - (m_b \cdot d)^2$, $\bar{M}_{12} = M_{12}m_b - (m_b sin(\Theta))(m_b \cdot d)$, $\bar{M}_{13} = -M_{12}(m_b \cdot d) + (m_b sin(\Theta))(J_t + m_b Y^2)$, and also $\bar{M}_{21} = M_{21} \cdot m_b - (m_b sin(\Theta))(m_b \cdot d)$, $\bar{M}_{22} = -M_{11}m_b - (m_b sin(\Theta))^2$, $\bar{M}_{23} = -M_{11}m_b d - M_{12}m_b sin(\Theta)$, $\bar{M}_{31} = M_{12}m_b d + (J_t + m_b Y^2)(m_b sin(\Theta))$, $\bar{M}_{32} = -M_{11}m_b d + M_{12}(m_b sin(\Theta))$, $\bar{M}_{33} = M_{11}(J_t + m_b Y^2) - M_{12}^2$ while the determinant of inertia matrix is $detM = M_{11}\bar{M}_{11} - M_{12}\bar{M}_{12} + M_{13}\bar{M}_{13}$.

About the product $(H+C)\dot{q}$ it holds that

$$(H+C)\dot{q} = \begin{pmatrix} C_{11} & C_{12} + H_{12}\dot{\Theta} & -2m_h\dot{\Theta}cos(\Theta) \\ C_{12} & C_{22} + 2m_h Y\dot{Y} & 0 \\ 0 & -m_h Y\Theta & C_y \end{pmatrix}\begin{pmatrix} \dot{X} \\ \dot{\Theta} \\ \dot{Y} \end{pmatrix} \tag{14}$$

which is also written as

$$(H+C)\dot{q} = \begin{pmatrix} C_{11}\dot{X} & (C_{12} + H_{12}\dot{\Theta})\dot{\Theta} & (-2m_h\dot{\Theta}cos(\Theta))\dot{Y} \\ C_{12}\dot{X} & (C_{22} + 2m_h Y\dot{Y})\dot{\Theta} & 0 \\ 0 & (-m_h Y\Theta)\dot{\Theta} & C_y\dot{Y} \end{pmatrix} = \begin{pmatrix} \bar{h}_1 \\ \bar{h}_2 \\ \bar{h}_3 \end{pmatrix} \tag{15}$$

Moreover, about the product $-M^{-1}(H+G)\dot{q}$ it holds that

$$M^{-1}(H+C)\dot{q} = \frac{1}{detM}\begin{pmatrix} \bar{M}_{11} & -\bar{M}_{21} & \bar{M}_{31} \\ -\bar{M}_{12} & \bar{M}_{22} & -\bar{M}_{22} \\ \bar{M}_{13} & -\bar{M}_{23} & \bar{M}_{33} \end{pmatrix}\begin{pmatrix} \bar{h}_1 \\ \bar{h}_2 \\ \bar{h}_3 \end{pmatrix} \tag{16}$$

which is also written as

$$M^{-1}(H+C)\dot{q} = \frac{1}{detM}\begin{pmatrix} \bar{M}_{11}\bar{h}_1 - \bar{M}_{21}\bar{h}_2 + \bar{M}_{31}\bar{h}_3 \\ -\bar{M}_{12}\bar{h}_1 + \bar{M}_{22}\bar{h}_2 - \bar{M}_{22}\bar{h}_3 \\ \bar{M}_{13}\bar{h}_1 - \bar{M}_{23}\bar{h}_2 + \bar{M}_{33}\bar{h}_3 \end{pmatrix} \tag{17}$$

Additionally, about the product $-M^{-1}Kq$ it holds that

$$M^{-1}Kq = \frac{1}{detM}\begin{pmatrix} \bar{M}_{11} & -\bar{M}_{21} & \bar{M}_{31} \\ -\bar{M}_{12} & \bar{M}_{22} & -\bar{M}_{32} \\ \bar{M}_{13} & -\bar{M}_{23} & \bar{M}_{33} \end{pmatrix}\begin{pmatrix} 0 \\ K_{22}\Theta \\ 0 \end{pmatrix} = \frac{1}{detM}\begin{pmatrix} -\bar{M}_{21}K_{22}\Theta \\ \bar{M}_{22}K_{22}\Theta \\ -\bar{M}_{23}K_{22}\Theta \end{pmatrix} = \frac{1}{detM}\begin{pmatrix} -\bar{M}_{21}\bar{k}_1 \\ \bar{M}_{22}\bar{k}_2 \\ -\bar{M}_{23}\bar{k}_3 \end{pmatrix} \tag{18}$$

where $\bar{k}_1 = \bar{k}_2 = \bar{k}_3 = K_{22}\Theta$. Consequently it holds that the aggregate term $-M^{-1}(H+C)\dot{q} - M^{-1}Kq$ takes the form

$$-M^{-1}(H+C)\dot{q} - M^{-1}Kq = \begin{pmatrix} -\bar{M}_{11}\bar{h}_1 + \bar{M}_{21}\bar{h}_2 - \bar{M}_{31}\bar{h}_3 + \bar{M}_{21}\bar{k}_1 \\ \bar{M}_{12}\bar{h}_1 - \bar{M}_{22}\bar{h}_2 + \bar{M}_{32}\bar{h}_3 - \bar{M}_{22}\bar{k}_2 \\ -\bar{M}_{13}\bar{h}_1 + \bar{M}_{23}\bar{h}_2 - \bar{M}_{33}\bar{h}_3 + \bar{M}_{23}\bar{k}_3 \end{pmatrix} \tag{19}$$

Additionally, about the control inputs gain matrix of the dual-drive gantry crane it holds that

$$M^{-1}A_f = \frac{1}{detM}\begin{pmatrix} \bar{M}_{11} & -\bar{M}_{21} & \bar{M}_{31} \\ -\bar{M}_{12} & \bar{M}_{2}2 & -barM_{32} \\ \bar{M}_{13} & -\bar{M}_{23} & \bar{M}_{33} \end{pmatrix}\begin{pmatrix} 1 & 1 & 0 \\ \frac{L_b}{2} & -\frac{L_b}{2} & 0 \\ 0 & 0 & 1 \end{pmatrix} \tag{20}$$

and by defining as $L_{b_1} = \frac{L_b}{2}$ the previous equation gives

$$M^{-1}A_f = \frac{1}{detM} = \frac{1}{detM}\begin{pmatrix} \bar{M}_{11} - L_{b_1}\bar{M}_{21} & \bar{M}_{11} + L_{b_1}\bar{M}_{21} & M_{31} \\ -\bar{M}_{12} + L_{b_1}\bar{M}_{22} & -\bar{M}_{12} - L_{b_1}\bar{M}_{22} & -M_{32} \\ \bar{M}_{13} - L_{b_1}\bar{M}_{23} & \bar{M}_{13} + L_{b_1}\bar{M}_{23} & \bar{M}_{33} \end{pmatrix} \tag{21}$$

Consequently, the dynamic model of the dual-drive gantry crane is written as:

$$\begin{pmatrix} \ddot{X} \\ \ddot{\Theta} \\ \ddot{Y} \end{pmatrix} = \begin{pmatrix} \frac{-\bar{M}_{11}\bar{h}_1 + \bar{M}_{21}\bar{h}_2 - \bar{M}_{31}\bar{h}_3 + \bar{M}_{21}\bar{k}_1}{detM} \\ \frac{\bar{M}_{12}\bar{h}_1 - \bar{M}_{22}\bar{h}_2 + \bar{M}_{32}\bar{h}_3 - \bar{M}_{22}\bar{k}_2}{detM} \\ \frac{-\bar{M}_{13}\bar{h}_1 + \bar{M}_{23}\bar{h}_2 - \bar{M}_{33}\bar{h}_3 - \bar{M}_{23}\bar{k}_3}{detM} \end{pmatrix} + \begin{pmatrix} \frac{\bar{M}_{11} - L_{b_1}\bar{M}_{21}}{detM} & \frac{\bar{M}_{11} + L_{b_1}\bar{M}_{21}}{detM} & \frac{M_{31}}{detM} \\ \frac{-\bar{M}_{12} + L_{b_1}\bar{M}_{2}2}{detM} & \frac{-\bar{M}_{12} - L_{b_1}\bar{M}_{22}}{detM} & \frac{-M_{32}}{detM} \\ \frac{\bar{M}_{13} - L_{b_1}\bar{M}_{23}}{detM} & \frac{\bar{M}_{13} + L_{b_1}\bar{M}_{23}}{detM} & \frac{\bar{M}_{33}}{detM} \end{pmatrix}\begin{pmatrix} F_1 \\ F_2 \\ F_y \end{pmatrix} \tag{22}$$

About the forces which are generated by the PMLSM actuators it holds that

$$F_1 = \frac{3\pi n_{p1}}{m_1 + m_b + m_h}\frac{\lambda_{pm_1}}{2\tau 1} i_{q1} \Rightarrow F_1 = w_1 i_{q1} \tag{23}$$

$$F_2 = \frac{3\pi n_{p2}}{m_2 + m_b + m_h}\frac{\lambda_{pm_2}}{2\tau 2} i_{q2} \Rightarrow F_2 = w_2 i_{q2} \tag{24}$$

$$F_y = \frac{3\pi n_{p3}}{m_h}\frac{\lambda_{pm_3}}{2\tau 3} i_{q3} \Rightarrow F_y = w_3 i_{q3} \tag{25}$$

The currents of the PMLSMs are given by the following equations:

First PMLSM of the rigid beam

$$\dot{i}_{q1} = -i_{q1}\frac{R_{s1}}{L_{q1}} - \frac{n_{p1}\pi\dot{X}_1}{L_{q1}\tau_1}(L_{d1}i_{d1} + \lambda_{pm1}) + \frac{1}{L_{q1}}v_{q1} \tag{26}$$

$$\dot{i}_{d1} = -i_{d1}\frac{R_{s1}}{L_{d1}} - \frac{n_{p1}\pi\dot{X}_1}{L_{d1}\tau_1}(L_{q1}i_{q1}) + \frac{1}{L_{d1}}v_{d1} \tag{27}$$

Second PMLSM of the rigid beam

$$\dot{i}_{q2} = -i_{q2}\frac{R_{s2}}{L_{q2}} - \frac{n_{p2}\pi\dot{X}_2}{L_{q2}\tau_2}(L_{d2}i_{d2} + \lambda_{pm2}) + \frac{1}{L_{q2}}v_{q2} \tag{28}$$

$$\dot{i}_{d2} = -i_{d2}\frac{R_{s2}}{L_{d2}} - \frac{n_{p2}\pi\dot{X}_2}{L_{d2}\tau_2}(L_{q2}i_{q2}) + \frac{1}{L_{d2}}v_{d2} \tag{29}$$

Third PMLSM of the load

$$\dot{i}_{q3} = -i_{q3}\frac{R_{s3}}{L_{q3}} - \frac{n_{p3}\pi\dot{Y}}{L_{q3}\tau_3}(L_{d3}i_{d3} + \lambda_{pm3}) + \frac{1}{L_{q3}}v_{q3} \tag{30}$$

$$\dot{i}_{d3} = -i_{d3}\frac{R_{s3}}{L_{d3}} - \frac{n_{p3}\pi\dot{Y}}{L_{d3}\tau_3}(L_{q3}i_{q3}) + \frac{1}{L_{d3}}v_{d3} \tag{31}$$

Besides, from Eq. (1) it holds

$$\begin{array}{ll} X_1 = X + L_{b1}\Theta & \dot{X}_1 = \dot{X} + L_{b1}\dot{\Theta} \\ X_2 = X - L_{b2}\Theta & \dot{X}_2 = \dot{X} - L_{b2}\dot{\Theta} \end{array} \tag{32}$$

Next, the state-vector of the dual-drive gantry crane is defined as

$$\begin{array}{c} x = [x_1, x_2, x_3, x_4, x_5, x_6, x_7, x_8, x_9, x_{10}, x_{11}, x_{12}]^T \Rightarrow \\ x = [X.\Theta, Y, \dot{X}, \dot{\Theta}, \dot{Y}, i_{d1}, i_{q1}, i_{d2}, i_{q2}, i_{d3}, i_{q3}] \end{array} \tag{33}$$

while the control inputs vector is defined as

$$\begin{array}{c} u = [u_1, u_2, u_3, u_4, u_5, u_6]^T \Rightarrow \\ u = [v_{d1}, v_{q1}, v_{d2}, v_{q2}, v_{d3}, v_{q3}] \end{array} \tag{34}$$

Using this state-vector and control inputs vector notation, the dynamic model of the dual-drive gantry crane is written as follows

$$\dot{x}_1 = x_4 \tag{35}$$

$$\dot{x}_2 = x_5 \tag{36}$$

$$\dot{x}_3 = x_6 \tag{37}$$

$$\dot{x}_4 = \frac{-\bar{M}_{11}\bar{h}_1+\bar{M}_{21}\bar{h}_2-\bar{M}_{31}\bar{h}_3+\bar{M}_{21}\bar{k}_1}{detM} + \frac{\bar{M}_{11}-L_{b1}\bar{M}_{21}}{detM}w_1x_7 + \frac{\bar{M}_{11}+L_{b1}\bar{M}_{21}}{detM}w_2x_9 + \frac{\bar{M}_{31}}{detM}w_3x_{11} \tag{38}$$

$$\dot{x}_5 = \frac{\bar{M}_{12}\bar{h}_1-\bar{M}_{22}\bar{h}_2+\bar{M}_{32}\bar{h}_3-\bar{M}_{22}\bar{k}_2}{detM} + \frac{-\bar{M}_{12}+L_{b1}\bar{M}_{22}}{detM}w_1x_7 + \frac{-\bar{M}_{12}+L_{b1}\bar{M}_{22}}{detM}w_2x_9 + \frac{-\bar{M}_{32}}{detM}w_3x_{11} \tag{39}$$

$$\dot{x}_6 = \frac{-\bar{M}_{13}\bar{h}_1+\bar{M}_{23}\bar{h}_2-\bar{M}_{33}\bar{h}_3+\bar{M}_{23}\bar{k}_3}{detM} + \frac{\bar{M}_{13}-L_{b1}\bar{M}_{23}}{detM}w_1x_7 + \frac{\bar{M}_{13}+L_{b1}\bar{M}_{23}}{detM}w_2x_9 + \frac{\bar{M}_{33}}{detM}w_3x_{11} \tag{40}$$

$$\dot{x}_7 = -x_7\frac{R_{s1}}{L_{q1}} - \frac{n_{p1}\pi(x_4+L_{b1}x_5)}{L_{q1}\tau_1}(L_{d1}x_8 + \lambda_{pm1}) + \frac{1}{L_{q1}}u_1 \tag{41}$$

$$\dot{x}_8 = -x_8\frac{R_{s1}}{L_{d1}} - \frac{n_{p1}\pi(x_4+L_{b1}x_5)}{L_{d1}\tau_1}(L_{q1}x_7) + \frac{1}{L_{d1}}u_2 \tag{42}$$

$$\dot{x}_9 = -x_9\frac{R_{s2}}{L_{q2}} - \frac{n_{p2}\pi(x_4-L_{b1}x_5)}{L_{q2}\tau_2}(L_{d2}x_{10} + \lambda_{pm2}) + \frac{1}{L_{q2}}u_3 \tag{43}$$

$$\dot{x}_{10} = -x_{10}\frac{R_{s2}}{L_{d2}} - \frac{n_{p2}\pi(x_4-L_{b1}x_5)}{L_{d2}\tau_2}(L_{q2}x_9) + \frac{1}{L_{d2}}u_4 \tag{44}$$

$$\dot{x}_{11} = -x_{11}\frac{R_{s3}}{L_{q3}} - \frac{n_{p3}\pi x_6}{L_{q3}\tau_3}(L_{d3}x_{12} + \lambda_{pm3}) + \frac{1}{L_{q3}}u_5 \tag{45}$$

$$\dot{x}_{12} = -x_{12}\frac{R_{s3}}{L_{d3}} - \frac{n_{p3}\pi x_6}{L_{d3}\tau_3}(L_{q3}x_{11}) + \frac{1}{L_{d3}}u_6 \tag{46}$$

As a result of the above, the state-space model of the dual-drive gantry crane can be also written in the following matrix form:

$$\begin{pmatrix} \dot{x}_1 \\ \dot{x}_2 \\ \dot{x}_3 \\ \dot{x}_4 \\ \dot{x}_5 \\ \dot{x}_6 \\ \dot{x}_7 \\ \dot{x}_8 \\ \dot{x}_9 \\ \dot{x}_{10} \\ \dot{x}_{11} \\ \dot{x}_{12} \end{pmatrix} = \begin{pmatrix} x_4 \\ x_5 \\ x_6 \\ f_{4a} + f_{4b}w_1x_7 + f_{4c}w_2x_9 + f_{4d}w_3x_{11} \\ f_{5a} + f_{5b}w_1x_7 + f_{5c}w_2x_9 + f_{5d}w_3x_{11} \\ f_{6a} + f_{6b}w_1x_7 + f_{6c}w_2x_9 + f_{6d}w_3x_{11} \\ f_7 \\ f_8 \\ f_9 \\ f_{10} \\ f_{11} \\ f_{11} \end{pmatrix} + \begin{pmatrix} 0 & 0 & 0 & 0 & 0 & 0 \\ 0 & 0 & 0 & 0 & 0 & 0 \\ 0 & 0 & 0 & 0 & 0 & 0 \\ 0 & 0 & 0 & 0 & 0 & 0 \\ 0 & 0 & 0 & 0 & 0 & 0 \\ 0 & 0 & 0 & 0 & 0 & 0 \\ g_{7,1} & 0 & 0 & 0 & 0 & 0 \\ 0 & g_{8,2} & 0 & 0 & 0 & 0 \\ 0 & 0 & g_{9,3} & 0 & 0 & 0 \\ 0 & 0 & 0 & g_{10,4} & 0 & 0 \\ 0 & 0 & 0 & 0 & g_{11,5} & 0 \\ 0 & 0 & 0 & 0 & 0 & g_{12,6} \end{pmatrix} \begin{pmatrix} u_1 \\ u_2 \\ u_3 \\ u_4 \\ u_5 \\ u_6 \end{pmatrix} \tag{47}$$

where the drift vector of the state-space model comprises the following functions:
$f_{4a} = \frac{-\bar{M}_{11}\bar{h}_1 + \bar{M}_{21}\bar{h}_2 - \bar{M}_{31}\bar{h}_3 + \bar{M}_{21}\bar{k}_1}{detM}$, $f_{4b} = \frac{\bar{M}_{11} - L_{b1}\bar{M}_{21}}{detM}$, $f_{4c} = \frac{\bar{M}_{11} + L_{b1}\bar{M}_{21}}{detM}$, $f_{4d} = \frac{\bar{M}_{31}}{detM}w_3x_{11}$.

$f_{5a} = \frac{\bar{M}_{12}\bar{h}_1 - \bar{M}_{22}\bar{h}_2 + \bar{M}_{32}\bar{h}_3 - \bar{M}_{22}\bar{k}_2}{detM}$, $f_{5b} = \frac{-\bar{M}_{12} + L_{b1}\bar{M}_{22}}{detM}$, $f_{5c} = \frac{-\bar{M}_{12} + L_{b1}\bar{M}_{22}}{detM}$, $f_{5d} = \frac{-\bar{M}_{32}}{detM}$.

$f_6a = \frac{-\bar{M}_{13}\bar{h}_1 + \bar{M}_{23}\bar{h}_2 - \bar{M}_{33}\bar{h}_3 + \bar{M}_{23}\bar{k}_3}{detM}$, $f_{6b} = \frac{\bar{M}_{13} - L_{b1}\bar{M}_{23}}{detM}$, $f_{6c} = \frac{\bar{M}_{13} + L_{b1}\bar{M}_{23}}{detM}$, $f_{6d} = \frac{\bar{M}_{33}}{detM}$

$f_7 = -x_7\frac{R_{s1}}{L_{q1}} - \frac{n_{p1}\pi(x_4 + L_{b1}x_5)}{L_{q1}\tau_1}(L_{d1}x_8 + \lambda_{pm1})$, $f_8 = -x_8\frac{R_{s1}}{L_{d1}} - \frac{n_{p1}\pi(x_4 + L_{b1}x_5)}{L_{d1}\tau_1}(L_{q1}x_7)$, $f_9 = -x_9\frac{R_{s2}}{L_{q2}} - \frac{n_{p2}\pi(x_4 - L_{b1}x_5)}{L_{q2}\tau_2}(L_{d2}x_{10} + \lambda_{pm2})$, $f_{10} = -x_{10}\frac{R_{s2}}{L_{d2}} - \frac{n_{p2}\pi(x_4 - L_{b1}x_5)}{L_{d2}\tau_2}(L_{q2}x_9)$, $f_{11} = -x_{11}\frac{R_{s3}}{L_{q3}} - \frac{n_{p3}\pi x_6}{L_{q3}\tau_3}(L_{d3}x_{12} + \lambda_{pm3})$ and $f_{12} = -x_{12}\frac{R_{s3}}{L_{d3}} - \frac{n_{p3}\pi x_6}{L_{d3}\tau_3}(L_{q3}x_{11})$.

Finally, the state-space model of the dual-drive gantry crane is written in the following concise nonlinear affine-in-the-input state-space form:

$$\dot{x} = f(x) + g(x)u \tag{48}$$

where $x \in R^{12\times 1}$, $f(x) \in R^{12\times 1}$, $g(x) \in R^{12\times 6}$, and $u \in R^{6\times 1}$.

3 Differential flatness properties of the dual-drive H-type gantry crane

The dynamic model of the dual-drive H-type is differentially flat, with flat outputs vector

$$\begin{gathered} Y = [x_1, x_2, x_3, x_8, x_{10}, x_{12}]^T \Rightarrow \\ Y = [X, \Theta, Y, i_{d1}, , i_{d2}, i_{d3}]^T \end{gathered} \tag{49}$$

The state-space model of the dual-drive gantry-crane given in Eq. (47) comprises 12 state equations. From the first three rows of the state-space model one has

$$\begin{aligned} \dot{x}_1 = x_4 \Rightarrow x_4 = \tilde{h}_4(Y, \dot{Y}) \\ \dot{x}_2 = x_4 \Rightarrow x_5 = \tilde{h}_5(Y, \dot{Y}) \\ \dot{x}_3 = x_4 \Rightarrow x_6 = \tilde{h}_4(Y, \dot{Y}) \end{aligned} \tag{50}$$

which signifies that state variables x_4, x_5, x_6 are differential functions of the flat outputs of the system.

Next, from the fourth, firth and sixth rows of the state-space model one has

$$\begin{pmatrix} \dot{x}_4 \\ \dot{x}_5 \\ \dot{x}_6 \end{pmatrix} = \begin{pmatrix} f_{4a} \\ f_{5a} \\ f_{6a} \end{pmatrix} + \begin{pmatrix} f_{4b}w_1 & f_{4c}w_2 & f_{4d}w_3 \\ f_{5b}w_1 & f_{5c}w_2 & f_{5d}w_3 \\ f_{6b}w_1 & f_{6c}w_2 & f_{6d}w_3 \end{pmatrix} \begin{pmatrix} x_7 \\ x_9 \\ x_{11} \end{pmatrix} \tag{51}$$

or equivalently

$$\begin{pmatrix} x_7 \\ x_9 \\ x_{11} \end{pmatrix} = \begin{pmatrix} f_{4b}w_1 & f_{4c}w_2 & f_{4d}w_3 \\ f_{5b}w_1 & f_{5c}w_2 & f_{5d}w_3 \\ f_{6b}w_1 & f_{6c}w_2 & f_{6d}w_3 \end{pmatrix}^{-1} \left[\begin{pmatrix} \dot{x}_4 \\ \dot{x}_5 \\ \dot{x}_6 \end{pmatrix} - \begin{pmatrix} f_{4a} \\ f_{5a} \\ f_{6a} \end{pmatrix} \right] \tag{52}$$

where functions $(f_{4a}, f_{4b}, f_{4c}, f_{4d})$, $(f_{5a}, f_{5b}, f_{5c}, f_{5d})$, and $(f_{6a}, f_{6b}, f_{6c}, f_{6d})$ are functions of state variables x_i $i = 1 \cdots 6$ and thus they are also differential functions of the flat outputs of the system. Consequently, one obtains about state variables x_7, x_9, x_{11}

$$\begin{aligned} x_7 &= \tilde{h}_7(Y, \dot{Y}) \\ x_9 &= \tilde{h}_9(Y, \dot{Y}) \\ x_{11} &= \tilde{h}_{11}(Y, \dot{Y}) \end{aligned} \tag{53}$$

which signifies that state variables x_7, x_9, x_{11} are differential functions of the flat outputs of the system. Moreover, from rows 7 to 12 of the state-space model of Eq. (47) one solves for the control inputs u_1 to u_6. This gives:

$$\begin{pmatrix} u_1 \\ u_2 \\ u_3 \\ u_4 \\ u_5 \\ u_6 \end{pmatrix} = \begin{pmatrix} g_{7,1} & 0 & 0 & 0 & 0 & 0 \\ 0 & g_{8,2} & 0 & 0 & 0 & 0 \\ 0 & 0 & g_{9,3} & 0 & 0 & 0 \\ 0 & 0 & 0 & g_{10,4} & 0 & 0 \\ 0 & 0 & 0 & 0 & g_{11,5} & 0 \\ 0 & 0 & 0 & 0 & 0 & g_{12,6} \end{pmatrix}^{-1} \left[\begin{pmatrix} \dot{x}_7 \\ \dot{x}_8 \\ \dot{x}_9 \\ \dot{x}_{10} \\ \dot{x}_{11} \\ \dot{x}_{12} \end{pmatrix} - \begin{pmatrix} f_7 \\ f_8 \\ f_9 \\ f_{10} \\ f_{11} \\ f_{12} \end{pmatrix} \right] \tag{54}$$

where x_8, x_{10}, x_{12} are flat outputs of the system, while all other variables and functions which appear in the fight part of Eq. (54) are differential functions of the flat outputs of the system. Therefore, the control inputs u_i $i = 1 \cdots 6$ are also differential functions of the flat outputs of the system, or

$$u_i = \tilde{h}_{u_i}(Y, \dot{Y}) \; i = 1, 2, \cdots, 6 \tag{55}$$

Consequently, the dynamic model of the dual-drive gantry crane is differentially flat. The differential flatness property is also an implicit proof of the system's controllability. It also demonstrates that the system is input-output linearizable through successive differentiations of its flat outputs. Finally, it allows for solving the setpoints definition problem. First, one defines setpoints in an unconstrained manner for the state variables which are also flat outputs of the system, that is for state variables x_1, x_2, x_3, x_8, x_{10} and x_{12}. For the rest of the state variables of the gantry crane x_4, x_5, x_6, x_7, x_9, x_{11} setpoints are chosen using the differential relations that connect these state variables to the system's flat outputs.

4 Flatness-based control in successive loops for the dual-drive H-type gantry crane

4.1 Proof of differential flatness properties for the chained subsystems

The state-space model of the dual-drive H-type gantry crane of Eq.(47) is decomposed into a series of subsystems which are connected in chained form:

The first subsystem comprises the rows 1 to 3 of the state-space model of Eq. (47), and the following sub-vectors and sub-matrices are defined about it:

$$x_{1,3} = \begin{pmatrix} x_1 \\ x_2 \\ x_3 \end{pmatrix} \quad f_{1,3} = \begin{pmatrix} 0 \\ 0 \\ 0 \end{pmatrix} \quad g_{1,3} = \begin{pmatrix} 1 & 0 & 0 \\ 0 & 1 & 0 \\ 0 & 0 & 1 \end{pmatrix} \quad v_1 = \begin{pmatrix} x_4 \\ x_5 \\ x_6 \end{pmatrix} \tag{56}$$

where $x_{1,3}$ is the state vector of the subsystem and v_1 is the virtual control inputs vector.

The second subsystem comprises rows 4 to 6 of the state-space model of Eq. (47), and the following sub-vectors and sub-matrices are defined about it:

$$x_{4,6} = \begin{pmatrix} x_4 \\ x_5 \\ x_6 \end{pmatrix} \quad f_{4,6} = \begin{pmatrix} f_{4a} \\ f_{4b} \\ f_{4c} \end{pmatrix} \quad g_{4,6} = \begin{pmatrix} f_{4b} & f_{4c} & f_{4d} \\ f_{5b} & f_{5c} & f_{5d} \\ f_{6b} & f_{6c} & f_{6d} \end{pmatrix} \quad v_2 = \begin{pmatrix} x_7 \\ x_9 \\ x_{11} \end{pmatrix} \tag{57}$$

where $x_{4,6}$ is the state vector of the subsystem and v_2 is the virtual control inputs vector.

The third subsystem comprises the rows 7 to 12 of the state-space model of Eq. (47), and the following sub-vectors and sub-matrices are defined about it:

$$x_{7,12} = \begin{pmatrix} x_7 \\ x_8 \\ x_9 \\ x_{10} \\ x_{11} \\ x_{12} \end{pmatrix} \quad f_{7,12} = \begin{pmatrix} f_7 \\ f_8 \\ f_9 \\ f_{10} \\ f_{11} \\ f_{12} \end{pmatrix} \quad g_{7,12} = \begin{pmatrix} g_{7,1} & 0 & 0 & 0 & 0 & 0 \\ 0 & g_{8,2} & 0 & 0 & 0 & 0 \\ 0 & 0 & g_{9,3} & 0 & 0 & 0 \\ 0 & 0 & 0 & g_{10,4} & 0 & 0 \\ 0 & 0 & 0 & 0 & g_{11,5} & 0 \\ 0 & 0 & 0 & 0 & 0 & g_{12,6} \end{pmatrix} \quad u = \begin{pmatrix} u_1 \\ u_2 \\ u_3 \\ u_4 \\ u_5 \\ u_6 \end{pmatrix} \tag{58}$$

where $x_{7,12}$ is the state vector of the third subsystem and u is the virtual control inputs vector.

Consequently, the initial state-space model of Eq. (47) is decomposed into the chain of the following three subsystems:

$$\dot{x}_{1,3} = f_{1,3}(x_{1,2}) + g_{1,3}(x_{1,3})v_1 \tag{59}$$

$$\dot{x}_{4,6} = f_{4,6}(x_{1,3}, x_{4,6}) + g_{4,6}(x_{1,3}, x_{4,6})v_2 \tag{60}$$

$$\dot{x}_{7,12} = f_{7,12}(x_{1,3}, x_{4,6}, x_{7,12}) + g_{7,12}(x_{1,3}, x_{4,6}, x_{7,12})u \tag{61}$$

It will be proven that each one of the subsystems of Eq. (59] to Eq. (61), if viewed independently, is differentially flat.

For the subsystem of Eq. (59) the flat outputs vector is $y_1 = x_{1,3}$, the virtual control inputs vector is $v_1 = x_{4,6}$ while $f_{1,3}(x_{1,3})$, $g_{1,3}(x_{1,3})$ are functions of $y_1 = x_{1,3}$. By solving Eq. (59) for v_1 one obtains

$$v_1 = g_{1,3}^{-1}(x_{1,3})[\dot{x}_{1,3} - f_{1,3}(x_{1,3})] \tag{62}$$

It can be seen that v_1 is also a differential function of the flat output y_1, therefore the subsystem of Eq. (59) is differentially flat.

For the subsystem of Eq. (60) the flat outputs vector is $y_2 = x_{4,6}$, the virtual control inputs vector is $v_2 = [x_7, x_9, x_{11}]^T$, while $x_{1,3}$ is considered to be a coefficients vector. Moreover $f_{4,6}(x_{1,3}, x_{4,6})$ and

$g_{4,6}(x_{1,3}, x_{4,6})$ are functions of the flat outputs vector $x_{4,6}$ and of the coefficients vector $x_{1,3}$. By solving Eq. (60) for v_2 one obtains

$$v_2 = g_{4,6}^{-1}(x_{1,3}, x_{4,6})[\dot{x}_{4,6} - f_{4,6}(x_{1,3}, x_{4,6})] \tag{63}$$

It can be seen that v_2 is also a differential function of the flat output y_2, therefore the subsystem of Eq. (60) is differentially flat.

For the subsystem of Eq. (61) the flat outputs vector is $y_3 = x_{7,12}$, the real control inputs vector is u, while $x_{1,3}$, $x_{4,6}$ are considered to be a coefficients vectors. Moreover $f_{7,12}(x_{1,3}, x_{4,6}, x_{7,12})$ and $g_{7,12}(x_{1,3}, x_{4,6}, x_{7,12})$ are functions of the flat outputs vector $x_{7,12}$ and of the coefficients vector $x_{1,3}$, $x_{4,6}$. By solving Eq. (61) for u one obtains

$$u = g_{7,12}^{-1}(x_{1,3}, x_{4,6}, x_{7,12})[\dot{x}_{7,12} - f_{7,12}(x_{1,3}, x_{4,6}, x_{7,12})] \tag{64}$$

It can be seen that u is also a differential function of the flat output y_3, therefore the subsystem of Eq. (61) is differentially flat.

4.2 Design of a multi-loop flatness-based controller

By proving that each one of the subsystems of Eq. (59) to Eq. (61) is differentially flat, one can infer that it can be brought into the input-output linearized form and that a stabilizing feedback controller can be designed about it through the inversion of its dynamics. The implementation of flatness-based control in successive loops is shown in Fig. 2

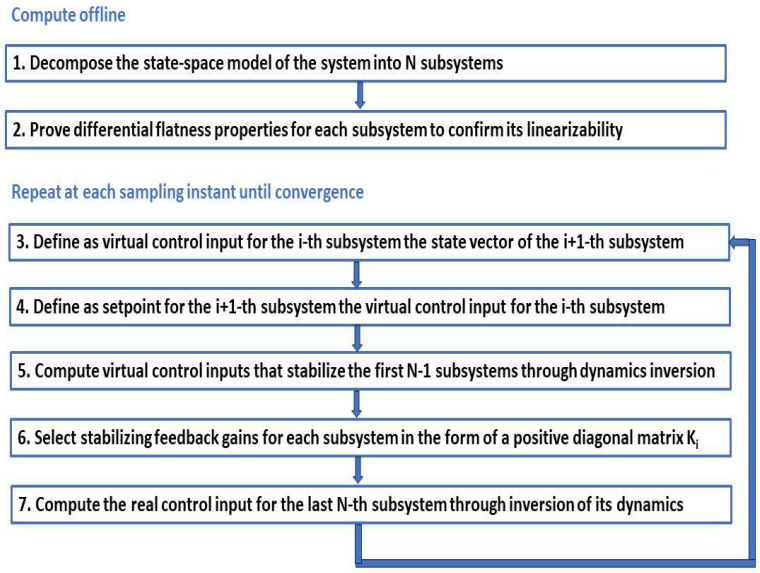

Figure 2: Implementation of flatness-based control in successive loops for the dual-drive H-type gantry crane

For the subsystem of Eq. (59) the stabilizing feedback controller is defined to be

$$v_1 = g_{1,3}^{-1}(x_{1,3})[\dot{x}_{1,3}^d - f_{1,3}(x_{1,3}) - K_1(x_{1,3} - x_{1,3}^d)] \tag{65}$$

where setpoint $x_{1,3}^d$ is selected without constraints, while $K_1 \in R^{3\times3}$ is a diagonal matrix with positive diagonal elements, that is $K_1 > 0$ and $K_{1,ii} > 0$ for $i = 1, 2, 3$. The virtual control input is $v_1 = x_{4,6}$ and becomes setpoint to the subsystem of Eq. (60), that is $v_1 = x_{4,6}^d$.

For the subsystem of Eq. (60) the stabilizing feedback controller is defined to be

$$v_2 = g_{4,6}^{-1}(x_{1,3}, x_{4,6})[\dot{x}_{4,6}^d - f_{4,6}(x_{1,3}, x_{4,6}) - K_2(x_{4,6} - x_{4,6}^d)] \tag{66}$$

where setpoint $x_{4,6}^d$ is selected without constraints, while $K_3 \in R^{3\times3}$ is a diagonal matrix with positive diagonal elements, that is $K_2 > 0$ and $K_{2,ii} > 0$ for $i = 1, 2, 3$. The virtual control input is $v_2 = [x_7, x_9, x_{11}]^T$ and jointly with the reference values $[x_8, x_{10}, x_{12}]^T$ becomes setpoint to the subsystem of Eq. (61), that is $x_{7,12}^d = [x_7^d, x_8^d, x_9^d, x_{10}^d, x_{11}^d, x_{12}^d]^T$.

For the subsystem of Eq. (61) the stabilizing feedback controller is defined to be

$$v_3 = g_{7,12}^{-1}(x_{1,3}, x_{4,6}, x_{7,12})[\dot{x}_{7,12}^d - f_{7,12}(x_{1,3}, x_{4,6}, x_{7,12}) - K_3(x_{7,12} - x_{7,12}^d)] \tag{67}$$

where setpoint $x_{7,12}^d = [x_7^d, x_8^d, x_9^d, x_{10}^d, x_{11}^d, x_{12}^d]^T$ has been defined above, while $K_3 \in R^{6\times6}$ is a diagonal matrix with positive diagonal elements, that is $K_3 > 0$ and $K_{3,ii} > 0$ for $i = 1, \cdots, 6$. The real control input is u and becomes setpoint to the subsystem of Eq. (60), that is $v_1 = x_{4,6}^d$.

By substituting the control input of Eq. (65) into the subsystem of Eq. (59) and by defining the tracking error variable $e_{1,3} = x_{1,3} - x_{1,3}^d$ one obtains

$$\begin{gathered} \dot{x}_{1,3} = f_{1,3} + g_{1,3} \cdot g_{1,3}^{-1}[\dot{x}_{1,3}^d - f_{1,3} - K_1(x_{1,3} - x_{1,3}^d)] \Rightarrow \\ (\dot{x}_{1,3} - \dot{x}_{1,3}^d) + K_1(x_{1,3} - x_{1,3}^d) = 0 \Rightarrow \dot{e}_{1,3} + K_1 e_{1,3} = 0 \Rightarrow \\ lim_{t\to\infty} e_{1,3}(t) = 0 \Rightarrow lim_{t\to\infty} x_{1,3}(t) = x_{1,3}^d(t) \end{gathered} \tag{68}$$

By substituting the control input of Eq. (66) into the subsystem of Eq. (60) and by defining the tracking error variable $e_{4,6} = x_{4,6} - x_{4,6}^d$ one obtains

$$\begin{gathered} \dot{x}_{4,6} = f_{4,6} + g_{4,6} \cdot g_{4,6}^{-1}[\dot{x}_{4,6}^d - f_{4,6} - K_2(x_{4,6} - x_{4,6}^d)] \Rightarrow \\ (\dot{x}_{4,6} - \dot{x}_{4,6}^d) + K_2(x_{4,6} - x_{4,6}^d) = 0 \Rightarrow \dot{e}_{4,6} + K_2 e_{4,6} = 0 \Rightarrow \\ lim_{t\to\infty} e_{4,6}(t) = 0 \Rightarrow lim_{t\to\infty} x_{4,6}(t) = x_{4,6}^d(t) \end{gathered} \tag{69}$$

By substituting the control input of Eq. (67) into the subsystem of Eq. (61) and by defining the tracking error variable $e_{7,12} = x_{7,12} - x_{7,12}^d$ one obtains

$$\begin{gathered} \dot{x}_{7,12} = f_{7,12} + g_{7,12} \cdot g_{7,12}^{-1}[\dot{x}_{7,12}^d - f_{7,12} - K_3(x_{7,12} - x_{7,12}^d)] \Rightarrow \\ (\dot{x}_{7,12} - \dot{x}_{7,12}^d) + K_3(x_{7,12} - x_{7,12}^d) = 0 \Rightarrow \dot{e}_{7,12} + K_3 e_{7,12} = 0 \Rightarrow \\ lim_{t\to\infty} e_{7,12}(t) = 0 \Rightarrow lim_{t\to\infty} x_{7,12}(t) = x_{7,12}^d(t) \end{gathered} \tag{70}$$

Consequently, all state variables of the dual-drive H-type gantry crane converge to the associated setpoints and the crane's control system is globally asymptotically stable.

Global asymptotic stability for the dual-drive H-type gantry crane can be also proven through Lyapunov analysis. To this end, the following Lyapunov function is defined:

$$V = \tfrac{1}{2}[e_{1,3}^T e_{1,3} + e_{4,6}^T e_{4,6} + e_{7,12}^T e_{7,12}] \tag{71}$$

By differentiating in time one obtains

$$\dot{V} = \tfrac{1}{2}2[e_{1,3}^T \dot{e}_{1,3} + e_{4,6}^T \dot{e}_{4,6} + e_{7,12}^T \dot{e}_{7,12}] \tag{72}$$

Next, by substituting in Eq. (72) the relations about the tracking error dynamics of Eq. (68), Eq. (69) and Eq. (70) one obtains

$$\dot{V} = \tfrac{1}{2}2[e_{1,3}^T(-K_1 e_{1,3}) + e_{4,6}^T(-K_2 e_{4,6}) + e_{7,12}^T(-K_3 e_{7,12})] \tag{73}$$

or equivalently

$$\dot{V} = -[e_{1,3}^T K_1 e_{1,3} + e_{4,6}^T K_2 e_{4,6} + e_{7,12}^T K_3 e_{7,12}] \tag{74}$$

Thus, finally it is concluded that

$$\dot{V} < 0 \; \forall \; e_{1,3} \neq 0, \; e_{4,6} \neq 0, \; e_{7,12} \neq 0 \tag{75}$$

while $V = 0$ iff $e_{1,3} = 0$, $e_{4,6} = 0$ and $e_{7,12} = 0$. Consequently, the first derivative of the system's Lyapunov function is always negative and the Lyapunov function V is a diminishing function which converges asymptotically to 0. Therefore $lim_{t\to\infty} e_{1,3}(t) = 0$, $lim_{t\to\infty} e_{4,6}(t) = 0$, $lim_{t\to\infty} e_{7,12}(t) = 0$ and the system is globally asymptotically stable.

5 Simulation tests

The performance of the flatness-based control method in successive loops for the dual-PMLSM-driven gantry crane. The obtained results are depicted in Fig. 3 to Fig. 18. They come to confirm that despite its simplicity the flatness-based control method in successive loops achieves fast and accurate tracking of reference setpoints under moderate variations of the control inputs. The selection of stabilizing values for the feedback gains of the controller is shown to be a straightforward and easy to follow procedure. Actually, to stabilize the gantry crane it suffices to select diagonal feedback gain matrices with positive diagonal elements. Thus, for the first subsystem the feedback gain matrix is $K_1 \in R^{3\times 3} > 0$ with diagonal elements $k_{1,ii} > 0$ for $i = 1, \cdots, 3$. Equivalently, for the second subsystem the feedback gain matrix is $K_2 \in R^{3\times 3} > 0$ with diagonal elements $k_{2,ii} > 0$ for $i = 1, \cdots, 3$. Finally, for the third subsystem the feedback gain matrix is $K_3 \in R^{6\times 6} > 0$ with diagonal elements $k_{3,ii} > 0$ for $i = 1, \cdots, 3$.

The flatness-based control method in successive loops provides also an automated procedure for selecting setpoints for the dynamic model of the dual-PMLSM-driven gantry crane. For the first subsystem and state variables $[x_1, x_2, x_3]^T$, $i = 1, 2, 3$, setpoints are chosen in an unconstrained manner. Next, the virtual control inputs of the first subsystem, that is state variables $v_1 = [x_4, x_5, x_6]^T$, become setpoints for the second subsystem. Additionally, the virtual control input for the second subsystem, that is $v_2 = [x_7, x_9, x_{11}]^T$, becomes part of the setpoints vector for the third subsystem. The rest of the setpoints vector for the third subsystem is complemented by setpoint variables $[x_8, x_{10}, x_{12}]$ which are selected in an unconstrained manner. Finally, it is noted that the transient performance of the control algorithm and the speed of convergence of the individual state variables to the associated setpoints is determined by the values which are assigned to the diagonal elements of the gain matrices K_i, $i = 1, 2, 3$.

6 Conclusions

In this article a novel nonlinear optimal control method has been developed for the dynamic model of a dual PMLSM-driven gantry crane. Such a type of cranes consists of a pair of permanent magnet linear synchronous motors arranged along the vertical axis and of a crossbeam along the horizontal axis which connects rigidly the two motors of the vertical axes. On the crossbeam a third linear motor is mounted

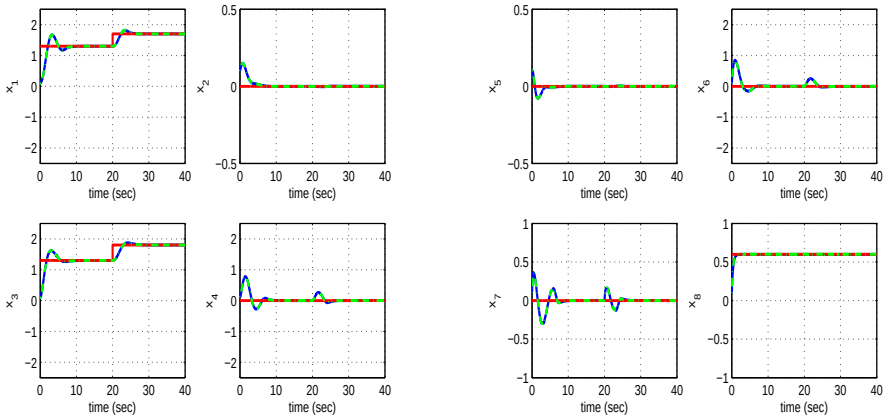

(a) **(b)**

Figure 3: Tracking of setpoint 1 by the dual-PMLSM-driven gantry crane with flatness-based control in successive loops (a) tracking of setpoints (red line) by the state variables of the gantry crane x_1 to x_4 (blue line) and estimates provided by the H-infinity Kalman Filter, (b) tracking of setpoints (red line) by the state variables of the gantry crane x_5 to x_8 (blue line) and estimates provided by the H-infinity Kalman Filter.

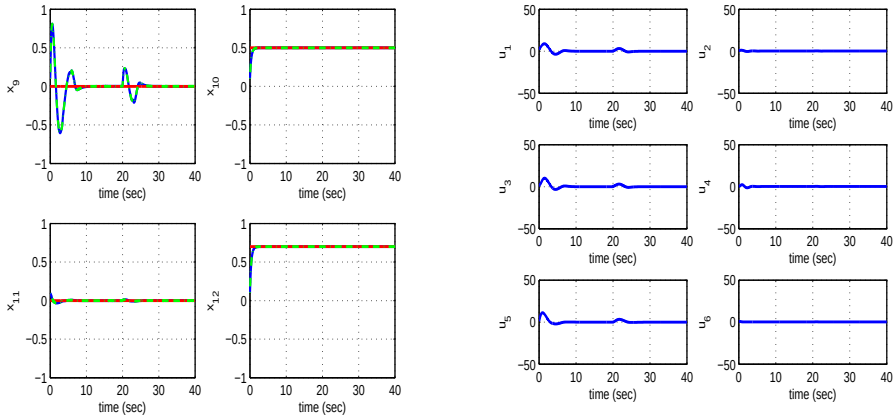

(a) **(b)**

Figure 4: Tracking of setpoint 1 by the dual-PMLSM-driven gantry crane with flatness-based control in successive loops (a) tracking of setpoints (red line) by the state variables of the gantry crane x_9 to x_{12} (blue line) and estimates provided by the H-infinity Kalman Filter, (b) variations of the control inputs of the gantry crane u_1 to u_6 (blue line).

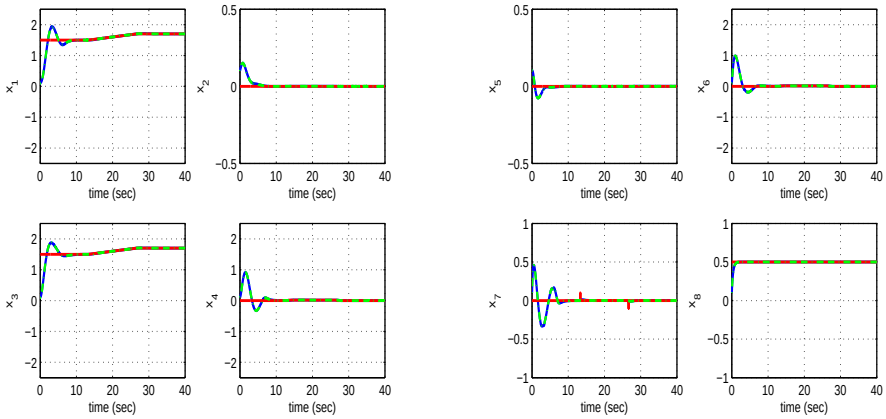

(a) **(b)**

Figure 5: Tracking of setpoint 2 by the dual-PMLSM-driven gantry crane with flatness-based control in successive loops (a) tracking of setpoints (red line) by the state variables of the gantry crane x_1 to x_4 (blue line) and estimates provided by the H-infinity Kalman Filter, (b) tracking of setpoints (red line) by the state variables of the gantry crane x_5 to x_8 (blue line) and estimates provided by the H-infinity Kalman Filter.

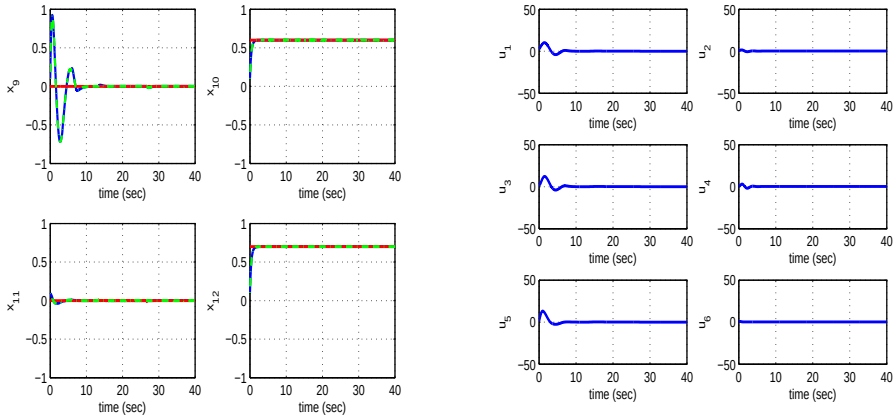

(a) **(b)**

Figure 6: Tracking of setpoint 2 by the dual-PMLSM-driven gantry crane with flatness-based control in successive loops (a) tracking of setpoints (red line) by the state variables of the gantry crane x_9 to x_{12} (blue line) and estimates provided by the H-infinity Kalman Filter, (b) variations of the control inputs of the gantry crane u_1 to u_6 (blue line).

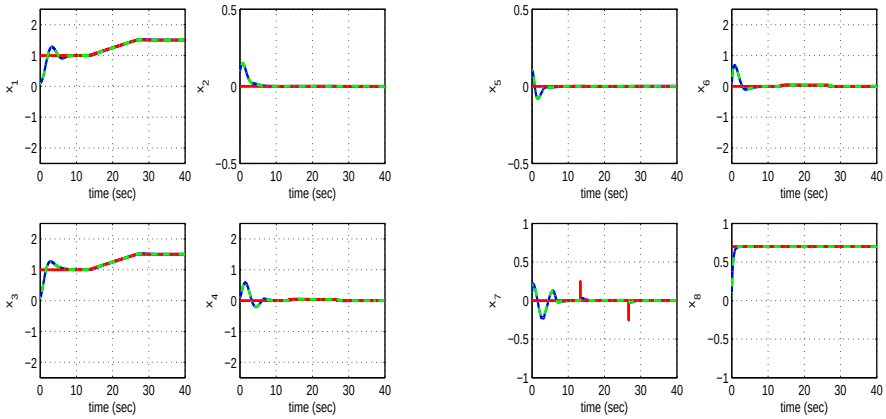

(a) **(b)**

Figure 7: Tracking of setpoint 3 by the dual-PMLSM-driven gantry crane with flatness-based control in successive loops (a) tracking of setpoints (red line) by the state variables of the gantry crane x_1 to x_4 (blue line) and estimates provided by the H-infinity Kalman Filter, (b) tracking of setpoints (red line) by the state variables of the gantry crane x_5 to x_8 (blue line) and estimates provided by the H-infinity Kalman Filter.

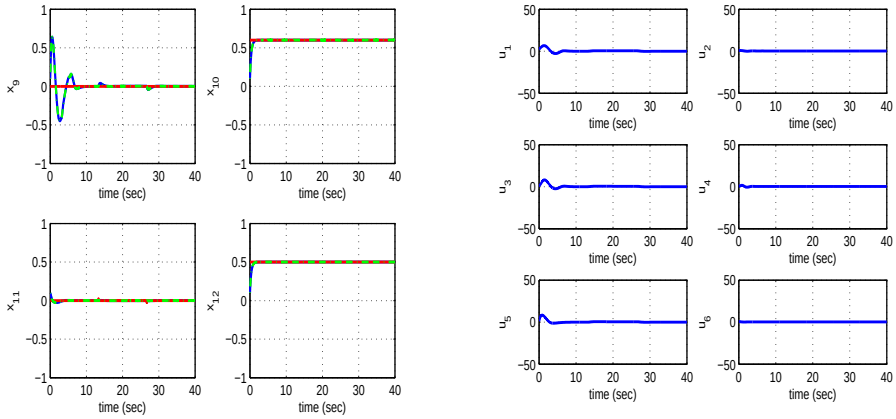

(a) **(b)**

Figure 8: Tracking of setpoint 3 by the dual-PMLSM-driven gantry crane with flatness-based control in successive loops (a) tracking of setpoints (red line) by the state variables of the gantry crane x_9 to x_{12} (blue line) and estimates provided by the H-infinity Kalman Filter, (b) variations of the control inputs of the gantry crane u_1 to u_6 (blue line).

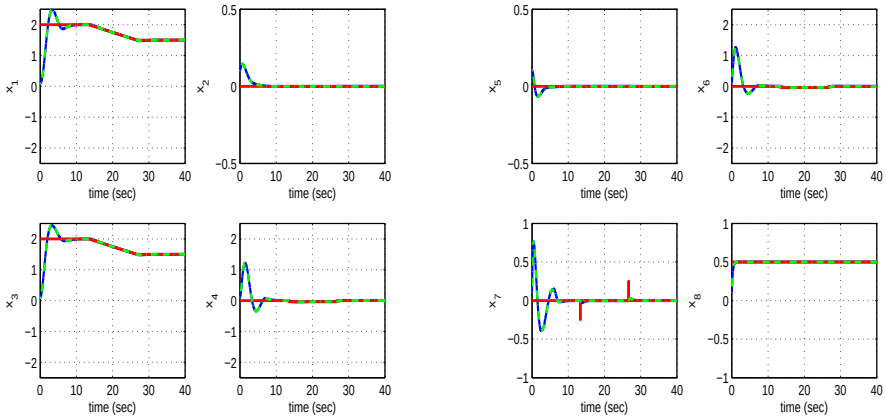

(a) **(b)**

Figure 9: Tracking of setpoint 4 by the dual-PMLSM-driven gantry crane with flatness-based control in successive loops (a) tracking of setpoints (red line) by the state variables of the gantry crane x_1 to x_4 (blue line) and estimates provided by the H-infinity Kalman Filter, (b) tracking of setpoints (red line) by the state variables of the gantry crane x_5 to x_8 (blue line) and estimates provided by the H-infinity Kalman Filter.

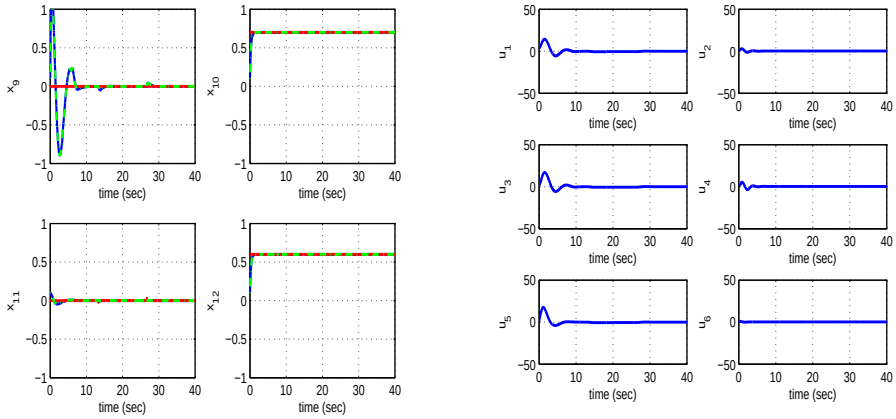

(a) **(b)**

Figure 10: Tracking of setpoint 4 by the dual-PMLSM-driven gantry crane with flatness-based control in successive loops (a) tracking of setpoints (red line) by the state variables of the gantry crane x_9 to x_{12} (blue line) and estimates provided by the H-infinity Kalman Filter, (b) variations of the control inputs of the gantry crane u_1 to u_6 (blue line).

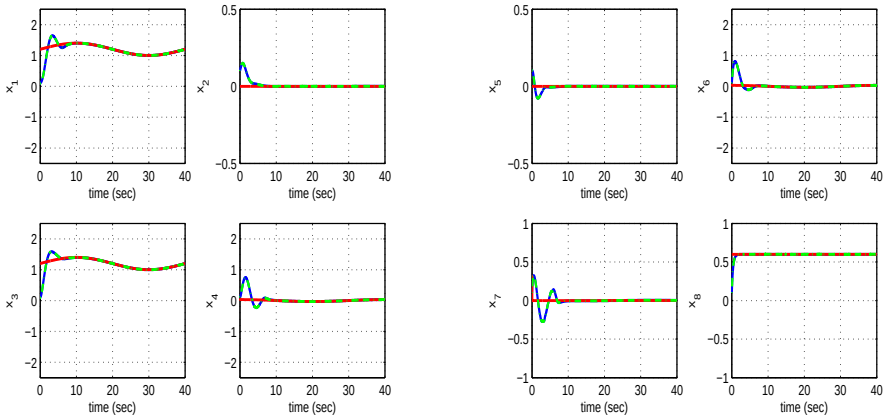

(a) **(b)**

Figure 11: Tracking of setpoint 5 by the dual-PMLSM-driven gantry crane with flatness-based control in successive loops (a) tracking of setpoints (red line) by the state variables of the gantry crane x_1 to x_4 (blue line) and estimates provided by the H-infinity Kalman Filter, (b) tracking of setpoints (red line) by the state variables of the gantry crane x_5 to x_8 (blue line) and estimates provided by the H-infinity Kalman Filter.

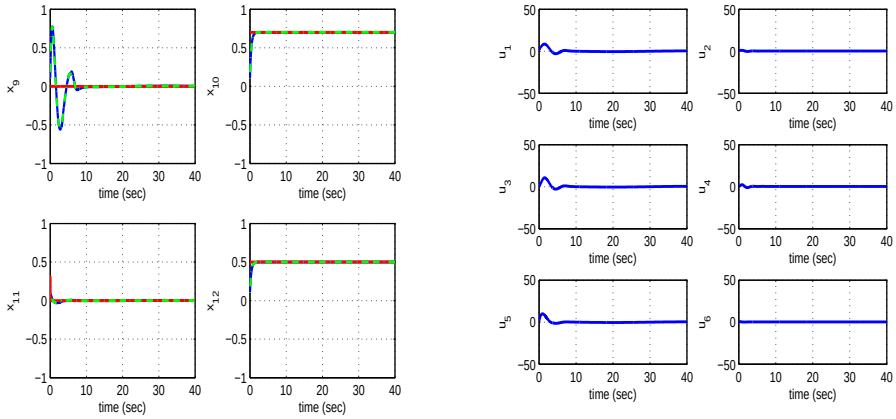

(a) **(b)**

Figure 12: Tracking of setpoint 5 by the dual-PMLSM-driven gantry crane with flatness-based control in successive loops (a) tracking of setpoints (red line) by the state variables of the gantry crane x_9 to x_{12} (blue line) and estimates provided by the H-infinity Kalman Filter, (b) variations of the control inputs of the gantry crane u_1 to u_6 (blue line).

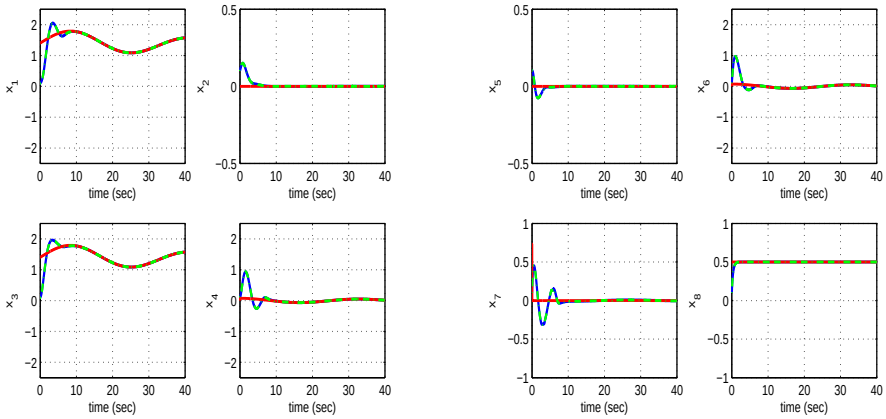

(a) **(b)**

Figure 13: Tracking of setpoint 6 by the dual-PMLSM-driven gantry crane with flatness-based control in successive loops (a) tracking of setpoints (red line) by the state variables of the gantry crane x_1 to x_4 (blue line) and estimates provided by the H-infinity Kalman Filter, (b) tracking of setpoints (red line) by the state variables of the gantry crane x_5 to x_8 (blue line) and estimates provided by the H-infinity Kalman Filter.

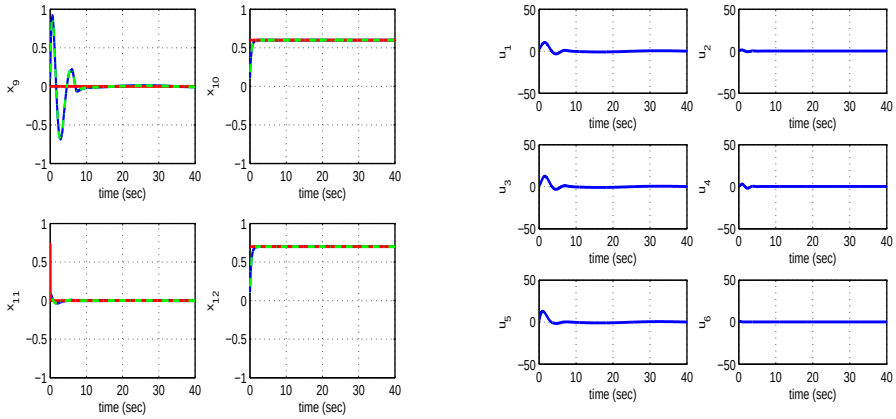

(a) **(b)**

Figure 14: Tracking of setpoint 6 by the dual-PMLSM-driven gantry crane with flatness-based control in successive loops (a) tracking of setpoints (red line) by the state variables of the gantry crane x_9 to x_{12} (blue line) and estimates provided by the H-infinity Kalman Filter, (b) variations of the control inputs of the gantry crane u_1 to u_6 (blue line).

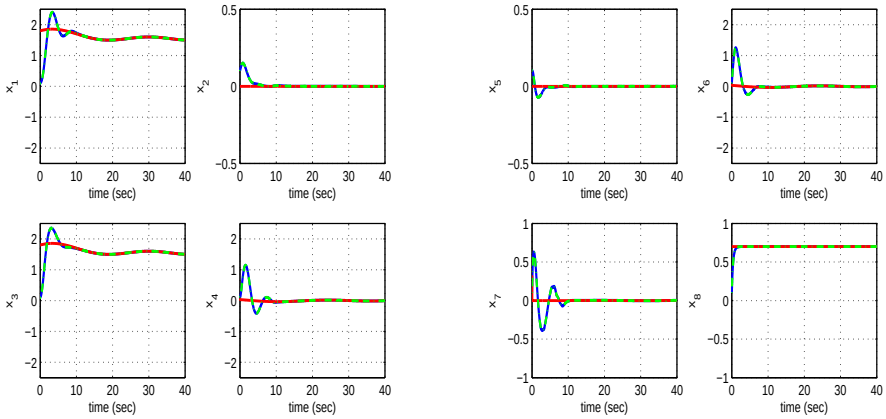

(a) **(b)**

Figure 15: Tracking of setpoint 7 by the dual-PMLSM-driven gantry crane with flatness-based control in successive loops (a) tracking of setpoints (red line) by the state variables of the gantry crane x_1 to x_4 (blue line) and estimates provided by the H-infinity Kalman Filter, (b) tracking of setpoints (red line) by the state variables of the gantry crane x_5 to x_8 (blue line) and estimates provided by the H-infinity Kalman Filter.

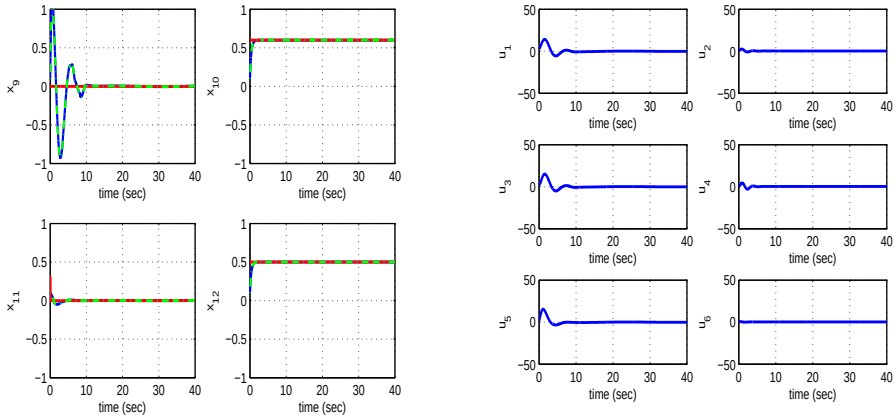

(a) **(b)**

Figure 16: Tracking of setpoint 7 by the dual-PMLSM-driven gantry crane with flatness-based control in successive loops (a) tracking of setpoints (red line) by the state variables of the gantry crane x_9 to x_{12} (blue line) and estimates provided by the H-infinity Kalman Filter, (b) variations of the control inputs of the gantry crane u_1 to u_6 (blue line).

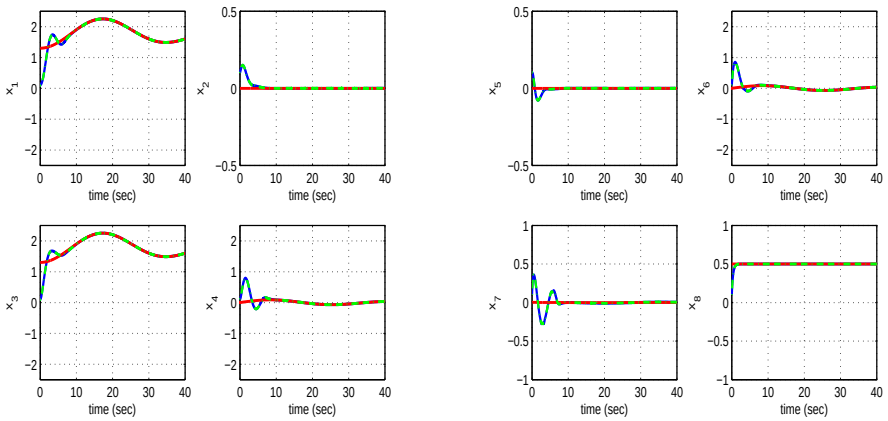

(a) **(b)**

Figure 17: Tracking of setpoint 8 by the dual-PMLSM-driven gantry crane with flatness-based control in successive loops (a) tracking of setpoints (red line) by the state variables of the gantry crane x_1 to x_4 (blue line) and estimates provided by the H-infinity Kalman Filter, (b) tracking of setpoints (red line) by the state variables of the gantry crane x_5 to x_8 (blue line) and estimates provided by the H-infinity Kalman Filter.

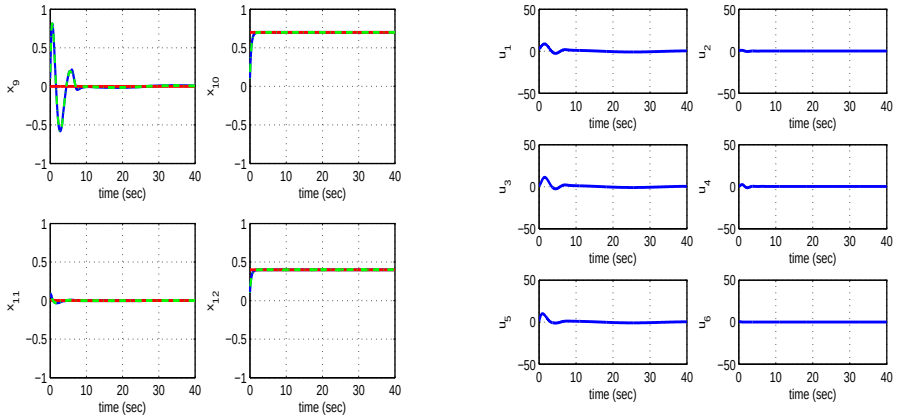

(a) **(b)**

Figure 18: Tracking of setpoint 8 by the dual-PMLSM-driven gantry crane with flatness-based control in successive loops (a) tracking of setpoints (red line) by the state variables of the gantry crane x_9 to x_{12} (blue line) and estimates provided by the H-infinity Kalman Filter, (b) variations of the control inputs of the gantry crane u_1 to u_6 (blue line).

which enables to move a load along the horizontal axis. For the reliable functioning of this crane complete synchronization of its motors is needed and this results into a complicated nonlinear control problem for the integrated dynamic model of the crane and the PMLSMs. It has been proven that the dynamic model of the dual PMLSM-driven gantry crane is differentially flat. Next, to achieve control and stabilization of the gantry crane's dynamics flatness-based controller in successive loops was designed. To this end, the dynamic model of the dual-PMLSM-driven gantry crane was decomposed into a series of subsystems which were connected in chained form. It was proven that, each one of these subsystems, if viewed independently is differentially flat. The state vector of the subsequent $i+1$-th subsystem was considered to be a virtual control input for the preceding i-th subsystem. Equivalently, the virtual control inputs vector of the preceding i-th subsystem was considered to be the setpoints vector of the subsequent $i+1$-th subsystem. From the last N-th subsystem the real control inputs of the gantry crane were computed by tracing backwards all preceding subsystems $N-1, \cdots, 1$.

Compared to nonlinear optimal control for the dual PMLSM-driven gantry crane, the flatness-based control method in successive loops is suboptimal because it does not include explicitly among the controller's objectives the minimization of the variations of the control inputs. However, despite its simplicity, the flatness-based control method in successive loops performs also remarkably well and achieves also fast and accurate tracking of setpoints by the state variables of the gantry crane. Using the local differential flatness properties of each one of the individual subsystems the design of a local stabilizing feedback controller becomes an easy procedure. It suffices (i) to perform inversion of the dynamics of each subsystem, as it is often done for input-output linearizable systems, (ii) the control input for each subsystem to comprise a diagonal feedback gains matrix with positive diagonal elements. The elimination of the state vector's tracking error and the global stability properties of this control scheme have been also proven through Lyapunov analysis. Finally, it is noteworthy that unlike global linearization-based control schemes the flatness-based control method in successive loops avoids any changes of state variables and state-space model transformations.

Acknowledgement: This research work has been partially supported by Grant Ref. 301022 'Nonlinear optimal and flatness-based control methods for complex dynamical systems' of the Unit of Industrial Automation of the Industrial Systems Institute. Besides, the authors, Pierluigi Siano and Mohammed Al-Numay acknowledge financial support from the Distinguished Scientist Fellowship Program, King Saud University, Riyadh, Saudi Arabia.

References

[1] G. Rigatos, Nonlinear control and filtering using differential flatnesss theory approaches: Applications to electromechanical systems, Springer, 2015

[2] G. Rigatos and E. Karapanou, Advances in applied nonlinear optimal control, Cambridge Scholars Publishing, 2020.

[3] G. Rigatos, M. Abbaszadeh and M.A. Hamida, Nonlinear control, estimation and fault diagnosis for electric power generation, traction and propulsion systems, Cambridge Scholars Publishing, 2023.

[4] G. Rigatos, Intelligent Renewable Energy Systems: Modelling and Control, Springer, 2016.

[5] G. Rigatos, M. Abbaszadeh, P. Siano, Control and estimation of dynamical nonlinear and partial differential equation systems: Theory and Applications, IET Publications, 2022

[6] J.Levine, Analysis and Control of Nonlinear Systems: A flatness-based approach, Springer 2009.

[7] M. Fliess and H. Mounier, Tracking control and π-freeness of infinite dimensional linear systems, In: G. Picci and D.S. Gilliam Eds.,Dynamical Systems, Control, Coding and Computer Vision, vol. 258, pp. 41-68, Birkhaüser, 1999.

[8] J. Villagra, B. d'Andrea-Novel, H. Mounier and M. Pengov, Flatness-based vehicle steering control strategy with SDRE feedback gains tuned via a sensitivity approach, IEEE Transactions on Control Systems Technology, vol. 15, pp. 554- 565, 2007.

[9] S. Bououden, D. Boutat, G. Zheng, J.P. Barbot and F. Kratz, A triangular canonical form for a class of 0-flat nonlinear systems, International Journal of Control, Taylor and Francis, vol. 84, no. 2, pp. 261-269, 2011.

[10] L. Menhour, B. d'Andre'a-Novel, M. Fliess and H. Mounier, Coupled nonlinear vehicle control: Flatness-based setting with algebraic estimation techniques, Control Engineering Practice, Elsevier, vol. 22, pp. 135–146, 2014

[11] F. Nicolaum W. Respondek and J.P. Barbot, How to minimally modify a dynamical system when constructing flat inputs, Internattional Journal of Robust and Nonlinear Control, J. Wiley, 2022.

[12] C. Letelier nd J.P. Barbot, Optimal flatness placement of sensors and actuators for controlling chaotic systemsm Chaos, AIP Publications, vol. 31, no. 10, article No 103114, 2021.

[13] H. Sira-Ramirez and S. Agrawal, Differentially Flat Systems, Marcel Dekker, New York, 2004.

[14] J. Lévine, On necessary and sufficient conditions for differential flatness, Applicable Algebra in Engineering, Communications and Computing, Springer, vol. 22, no. 1, pp. 47-90, 2011.

[15] F. Nicolau, W. Respondek and J.P. Barbot, Construction of flat inputs for mechanical systems, 7th IFAC Workshop on Lagrangian and Hamiltonian methods for nonlinear control, Berlin, Germany, OCt. 2021

[16] J.O. Limaverde Filho, E.C.R. Fortaleza and M.C.M. Campos, A derivative-free nonlinear Kalman Filtering approach using flat inputs, International Journal of Control, Taylor and Francis 2021.

[17] J.P. Barbot, M. Fliess and T. Floquet, An algebraic framework for the design of nonlinear observers with uknown inputs, IEEE CDC 2007, IEEE 46th Intl. Conference on Decision and Control, New Orleans, USA, Dec. 2007

[18] H. Khalil, Nonlinear Systems, Prentice Hall, 1996

[19] G.G. Rigatos and S.G. Tzafestas, Extended Kalman Filtering for Fuzzy Modelling and Multi-Sensor Fusion, Mathematical and Computer Modelling of Dynamical Systems, Taylor & Francis), vol. 13, pp. 251-266, 2007.

[20] M. Basseville and I. Nikiforov, Detection of abrupt changes: Theory and Applications, *Prentice-Hall*, 1993.

[21] G. Rigatos and Q. Zhang, Fuzzy model validation using the local statistical approach, Fuzzy Sets and Systems, Elsevier, vol. 60, no. 7, pp. 882-904,2009.

[22] G. Rigatos, P. Siano and N. Zervos, A new concept of flatness-based control of nonlinear dynamical systems, IEEE INDIN 2015, 13th IEEE Intl. Conf. on Industrial Informatics, Cambridge, UK, July 2015

[23] G. Rigatos, P. Siano, S Ademi and P. Wira, Flatness-based control of DC-DC converters implemented in successive loops, Electric Power Components and Systems, Taylor and Francis, vol. 46, no. 6, pp. 673-687, 2018.

[24] G. Rigatos, Flatness-based embedded control in successive loops for spark ignited engines, Journal of Physics, IOP Publications, Conference Series No 659, 012019, IFAC ACD 2015, Proc. of the 12th European Workshop on Advanced Control and Diagnosis.

[25] G. Rigatos and P. Siano, Flatness-based control in successive loops for Business Cycles of Finance Agents, Journal of Intelligent Industrial Systems, Springer, vol. 3, pp. 77-89, 2017

[26] Y. Liu, W. Su, C. Buccella and C. Cecati, Robust control of a dual-linear-motor-driven gantry stage for coordinated contouring tasks based on feed velocity, IEEE Transactions on Industrial Electronics, vol. 70, no. 6, pp. 6229-6238, 2023.

[27] Z. Liu, W. Lu, X. Yu, J.J. Rodriguez-Adina and H. Gao, Approximation-free robust synchronization control for dual-linear-motors-driven system with uncertainties and disturbances, IEEE Transactions on Industrial Electronics, vol. 69, no. 10, pp. 10500-10509, 2022.

[28] G. Zhang, H. Yi and W. Dou, Design of dual-drive vertical lift servo system and synchronous control performance analysis, IEEE/ASME Transactions on Mechatronics, vol. 25, no. 6, pp. 2927-2937, 2020.

[29] B. Xie, L. Lei, Y. Yan and Y. Lim, Advanced synchronous control fo dual parallel motion systems, IEEE Transactions on Industrial Electronics, vol. 70, no. 2, pp. 1270-1281, 2023.

[30] Z. Wang, C. Hu, Y. Zhu and L. Zhu, Prediction model-based-contouring error iterative precompensation scheme for position multiaxis motion systems, IEEE/ASME Transactions on Mechatronics, vol. 26, no. 5, pp. 2274, -2284, 2021.

[31] C. Hu, B. Yao and Q. Wang, Coordinated adaptive robust contouring controller design for an industrial biaxial precision gantry, IEEE Transactions on Mechatronics, vol. 15, no. 5, pp. 728-736, 2020.

[32] C.S. Teo, K.K. Tan, S.Y. Lim, S. Huang and E.B. Tay, Dynamic modelling and adaptive control of an H-type gantry stage, Mechatronics, Elsevier, vol. 17. pp. 361-367, 2007.

[33] J. Ma, S.L. Chen, N. Kamaldin, C.S. Teo, A. Tay, A. Al Mamun and K.K. Tan, Integrated mechatronic design in the flexure-linked dual-drive gantry by contrained Linear-Quadratic optimization, IEEE Transactions on Industrial Electronics, vol. 65, no. 3, pp. 2408-2418, 2018.

[34] J. Godovin, A. Maksakov, M. Shysh and S. Palis, Development of control for positioning of large gantry cranes, Mechanical Systems and Signal Processing, Elsevier, vol. 163, pp. 108199-108215, 2022.

[35] R.Chen, L. Yao, Z. Jiao and Y. Shang, Dynamic modeling and analysis of flexible H-type gantry stage: Journal of Sound and Vibration, Elsevier, vol. 439, pp. 144-155, 2019.

[36] P. Shi, W. Sun, X. Yang, I.J. Rudas and H.Gao, Master-slave synchronization control of dual-drive gantry stage with cogging force computation, IEEE Transactions on Systems, Man and Cybernetics, vol. 53, no. 1, pp. 216-226, 2023.

[37] W. Wang, J. Ma, Z. Chang, X. Li, A. Al Mamoun and T.M. Lee, Generalized iterative super-twisting sliding-mode control: A case study on flexure-joint, dual-drive H-gantry stage, IEEE ICIT 2021, IEEE 2021 Intl. Conference on Industrial Technology, Valencia, Spain, March 2021.

[38] N. Kamaldin, S.L. Chen, C.S. Teo, W. Lin, A. Tay and K.K. Tan, A novel adaptive jerk control woth application to large work-piece tracking on a flexure-linked dual drive gantry, IEEE Transactions on Industrial Electronics, vol. 66, no. 7, pp. 5353-5363, 2019.

[39] W.Wang, J. Ma, Z. Chang, X. li, C. da Silva and T.H. Lee, Global iterative sliding-mode control of an industrial biaxial gantry system for conturing motion tasks, IEEE/ASME Transactions on Mechatronics, vol. 27, no. 3, pp. 1617-1628, 2022.

[40] I. Garcia-Herreros, X. Kestelyn, J. Gomard, R. Coleman and P.J. Barre, Model-based decoupling control method for dual-drive gantry-stages: A case-study with experimental validation, Control Engineering Practice, Elsevier, vol. 21, pp. 298-307, 2013.

[41] I. Garcia-Herreros, X. Kestelyn, J. Gomard and P.J. Barre, Model-based control of a dual-drive H-type gantry stage on a decoupling base, IEEE ICIT 2010, IEEE 2010 Intl. Conference on Industrial Technology, Via del Mar, Chiel, March 2010.

[42] P. Shi, W. Sun and X. Yang, RBF neural network-based adaptive robust synchronization control of dual drive gantry stage with rotational coupling dynamics, IEEE Transactons on Automation Science and Engineering, vol. 20, no. 2, pp. 1059-1068, 2023.

[43] C. Li, Z. Chen and B. Yao, Adaptive robust synchronization control of a dual-linear-motor-driven gantry with rotational dynamics and accurate online parameter estimation, IEEE Transactions on Industrial Informatics, vol. 14, no. 7, pp. 2013-3022, 2018.

[44] Z. Chem, C. Li, B. Yao, M. Yuan and C. Yang, Integrated coordinated/synchronized contouring control of a dual-linear-motor-driven gantry, IEEE Transactions on Industrial Electronics, vol. 67, no. 5, pp. 3944-3954, 2020.

[45] C. Li, C. Li, Z. Chou and B. Yao, Advanced synchronization control of a dual-linear-motor-driven gantry with rotational dynamics, IEEE Transactions on Industrial Electronics, vol. 65, no. 9, pp. 7526-7535, 2018.

[46] F.J. Lin, P.H. Chen, C.J. Chen and Y.S. Lin, DSP-based cross-coupled synchronous control for dual linear motors via intelligent complementary slidinig-mode control, IEEE Transactions on Industrial Electronics, vol. 59, no. 2, pp. 1061-1073, 2012.

[47] P. Shi, X. Yu, X. Yang, J.J. Rodriguez-Andina, W. Sun and H. Gao, Composite adaptive synchronous control of dual-drive gantry stage with load measurement, IEEE Open Journal of the Industrial Electronics Society, vol. 4, pp. 63-74, 2023.

[48] C. Li, B. Yu and Q. Wang, Modelling and synchtonization control of a dual-drive industrial gantry stage, IEEE/ASME Transactions on Mechatroncis, vol. 23, no. 6, pp. 2340-2351, 2018.

[49] M.Y. Chen and J.S. Lu, High-precision motion control for a linear Permanent Magnet Iron-Core Synchronous Motor Drive in position platform, IEEE Transactions on Industrial Informatics, vol. 10, no.1, pp. 99-108, 2014.

[50] P.H. Chou, C.S. Chen and F.J. Lin, DSP-based synchronous control of dual linear motors via Sugeno-type fuzzy neural network compensator, Journal of the Franklin Institute, Elsevier,vol. 349, pp. 792-812, 2012

[51] J. Zheng, H. Wang, Z. Man, J. Lin and M. Fu, Robust motion control of a linear motor positioner using fast nonsingular terminal sliding-mode, IEEE/ASME Transactions on Mechatronics, vol. 20, no. 4, pp. 1743-1752, 2015.

[52] S.U. Chung, J.W. Kim, B.C. Woo, D.K. Hong, J.Y. Lee, Y.D. Chun, and D.H. Koo, Design and experimental validation of doubly salient permanent magnet linear synchronous motor for precision position control, Mechatronics, Elsevier, vol. 23, pp. 172-181, 2013

[53] M. Wang , L. Li and D. Pan, Detent force compensation for PMLSM systems based on structural design and control method combination, IEEE Transactions on Industrial Electronics, bol. 62, no. 11, pp. 6845-6854, 2015.

[54] B. Chappui, S. Gavin, L. Rigazzi snd M. Carpita, Speed control of a multi-phase active way linear mmotor based on back EMF estimator, IEEE Transactions on Industrial Electronics, vol. 62, no. 12, pp. 7299-7308, 2015.

[55] M.A.M. Cheema, J.E. Fletcher, M. Forshadmin, D. Xiao and M.F. Rahman, Combined speed and direct thrust force control of linear permanent-magnet synchronous motors with sensorless speed estimation using a sliding-mode control with integral action, IEEE Transactions on Industrial Electronics, vol. 64, no. 5, pp. 3489-3501, 2017.